IEEE Access
Multidisciplinary | Rapid Review | Open Access Journal

Received June 17, 2019, accepted June 22, 2019, date of publication June 27, 2019, date of current version July 17, 2019.

Digital Object Identifier 10.1109/ACCESS.2019.2925384

Holomorphic Embedding Based Continuation Method for Identifying Multiple Power Flow Solutions

DAN WU [1], (Member, IEEE), AND BIN WANG [2], (Member, IEEE)
[1]Laboratory for Information and Decision Systems, Massachusetts Institute of Technology, Cambridge, MA 02139, USA
[2]Department of Electrical and Computer Engineering, Texas A&M University, College Station, TX 77843, USA

Corresponding author: Bin Wang (binwang@tamu.edu)

This work was supported by the NSF CRISP Project 1735513.

ABSTRACT In this paper, we propose an efficient continuation method for locating multiple power flow solutions. We adopt the holomorphic embedding technique to represent solution curves as holomorphic functions in the complex plane. The holomorphicity, which provides global information of the curve at any regular point, enables large step sizes in the path-following procedure such that non-singular curve segments can be traversed with very few steps. When approaching singular points, we switch to the traditional predictor-corrector routine to pass through them and switch back afterward to the holomorphic embedding routine. We also propose a warm starter when switching to the predictor-corrector routine, i.e., a large initial step size based on the poles of the Padé approximation of the derived holomorphic function, since these poles reveal the locations of singularities on the curve. The numerical analysis and experiments on many standard IEEE test cases are presented, along with the comparison to the full predictor-corrector routine, confirming the efficiency of the method.

INDEX TERMS Power flow problem, holomorphic embedding, continuation.

I. INTRODUCTION

The electric power grid is a critical energy infrastructure for power generation, transmission, and distribution in modern society. The inherent nonlinearity of power grid introduces a great challenge to analyze its dynamical behaviors when subject to disturbances, especially when penetrated with a large amount of intermittent renewable energies. Identifying the region of attraction about the operating condition, i.e. a stable equilibrium point (SEP) of the underlying dynamical system, can significantly improve the situational awareness and, therefore, will be of great importance to avoid black-outs. Characterizing this region requires the knowledge of a special type of unstable equilibrium point (UEP) which is called the *type-1 UEP* [1], [2]. Determining them usually requires locating all nearby equilibria. In classical model [3], equilibria are solutions to the *power flow equations* [4]–[6].

A *high-voltage solution* in the range of $[0.9,\ 1.1]$[1] p.u. represents a steady state under which the system can be well-operated. This solution is usually the SEP in transient stability analysis, while other solutions are UEPs. For tree structured networks, the high-voltage solution is unique [7]. However, it is possible that mesh networks can have multiple high-voltage solutions with either circulated flow [8] or reversed power flow [9]. Although being avoided in the normal operations, circulated flow can happen during fault transients. Meanwhile, the reversal of power flow can become very common in future power grids as distributed energy resources (DER) keep penetrating into distribution networks. To better characterize stability region and to examine other high-voltage operating points, finding multiple power flow solutions plays a key role.

Nowadays a single high-voltage solution can be solved very efficiently. For example, systems with about 10,000 buses can be solved within a second [10]. However, the largest system that can be provably solved for all solutions is the 14-bus system [11]. The efficiency of solving a single high-voltage solution comes from the knowledge of a good initial guess for local solvers to converge. But it is rather hard to acquire appropriate initial guesses for other solutions. If using random seeds, the complexity increases

The associate editor coordinating the review of this manuscript and approving it for publication was Md Apel Mahmud.

[1]A more restricted range may be assumed to be $[0.95,\ 1.05]$ for transmission systems.

exponentially as the system size increases. Therefore, a systematic method is required to find these solutions. Early attempts to find multiple power flow solutions dates back to 1970s when [12] examined a 3-node system which admits 0, 2, 4 or 6 solutions. In 1989, [13], [14] introduced the probability-one homotopy continuation method to find all the complex-valued solutions to the power flow problem. The homotopy continuation method requires estimating the total number of solutions to the power flow problem, which is still an ongoing research. In 1982, [15] sharpened the solution number bound from the classic Bezout's bound, $2^{2N_{bus}-2}$, to a combinatorial bound, $C^{N_{bus}-1}_{2N_{bus}-2}$, where N_{bus} is the number of nodes in a power grid. Recently, [11] applied a polyhedral homotopy continuation method to completely solve the IEEE standard 14-bus system by the Bernstein-Khovanskii-Kushnirenko (BKK) bound which is sharper than the Bezout's bound. However, evaluating the BKK bound is very expensive. To further explore a simpler bound, [16] introduced the adjacent polytope bound, which is sharper than the BKK bound and more computable.

While progressive, the homotopy method usually ends up with a huge amount of complex-valued solutions which are fictitious power flow solutions. To only identify actual power flow solutions, [17] introduced the idea of curve design which connects different real solutions by some 1-dimensional curves. Following these curves power flow solutions can be reached one by one.[2] Though efficient, [19] provided a counter-example for [17]. To rectify their method, an elliptical formulation of the power flow problem is used in [20] to restrict the curve design on high dimensional ellipses. It helps solve all the standard IEEE test cases which can be verified by the homotopy method in a reasonable time,[3] including the counter-example in [19]. The existence and construction of elliptical formulation were provided in [21] and extended to the optimal power flow problem to find multiple local extrema for hard problems in [22].

The curve tracing routine performed in [20]–[22] is a traditional predictor-corrector algorithm which adopted a quadratic predictor [23], Newton's method for corrector, and an adaptive step-length control [24]. Many variations of the predictor-corrector algorithm exist, however, most of them depend only on the local information or previously solved points. To accelerate the curve tracing, in this paper, we design a new hybrid algorithm called the *holomorphic embedding based continuation* (HEBC) method to replace the traditional predictor-corrector algorithm during most of the curve tracing periods. It applies the holomorphic embedding technique to quickly pass through the non-singular curve segments by utilizing the global information of that curve, and uses a predictor-corrector routine to travel across singularities.

The holomorphic embedding method (HEM) was introduced by Trias [25] in 2012 as a new power flow solver. The basic idea is to parameterize a polynomial system by an extra free variable and acquires the solution curve information by power series. Early attempts to use parameterization and power series for solving power flows started with [26] and followed by [27], [28]. Recently, HEM was extended to some applications with different modelings [29]–[35]. In [36], different germs are designed for HEM, starting from each of these germs can trace up to one extra power flow solution. Unlike [36] which focuses on a special type of power flow solutions, this paper indistinguishably finds as many as possible. A restarted HELM was proposed in [37] to enhance the speed of HELM when computing the high-voltage solution, while a multi-stage scheme was proposed in [35] to eliminate the precision issue of HELM. Among the above developments, two features of HEM are particularly useful in our circumstance to improve searching efficiency. First, HEM can release us from local predictor-corrector scheme and provide with very long arc steps on the solution curve. This can largely reduce the burden of repeatedly solving linear systems in the corrector part. Moreover, the smallest real-valued pole of Padé approximation can be used to design an appropriate step length when passing through singular point. It avoids overly large step sizes to improve numerical stability, and keeps step sizes progressive to maintain efficiency.

The contributions of this paper are summarized below.

1) Showed an equivalent curve design for the elliptical formulation of the power flow problem.
2) Proposed a hybrid numerical continuation method HEBC for finding multiple power flow solutions.
3) Proposed a warm starter to quickly initiate the predictor-corrector routine for passing through singularities.
4) Showed that HEBC outperforms the traditional predictor-corrector algorithm [20] for all the tested cases.
5) Computed solution sets[4] for several large test cases which currently are intractable by homotopy continuation method or the similar.

II. DESCRIPTION OF POWER FLOW PROBLEM

Throughout this paper, we adopt the power flow formulation in rectangular coordinates.

A. POWER FLOW EQUATIONS IN RECTANGULAR COORDINATES

Consider a connected power grid with N_{bus} nodes. Let the node voltage vector be

$$\mathbf{V} := \mathbf{V}_d + j\mathbf{V}_q \tag{1}$$

[2]A very special type of test cases can be solved much more efficiently by some techniques from algebraic geometry. Interested readers are referred to [18]. However, there is no such efficient algebraic geometry method for solving a general power flow case at present.

[3]Currently, there is no rigorous theoretical guarantee to show that the elliptical formulation can always connect all the real solutions. It is an ongoing research.

[4]Several solution sets are available online [47].

where $\mathbf{V} \in \mathbb{C}^{N_{bus}}$; $\mathbf{V}_d \in \mathbb{R}^{N_{bus}}$ and $\mathbf{V}_q \in \mathbb{R}^{N_{bus}}$ are the real and imaginary parts of $\mathbf{V}$, respectively.

For the PQ bus, we have

$$V_k^\star \sum_{n=1}^{N_{bus}} Y_{n,k} V_n = S_k^\star \tag{2}$$

where V_k and V_n are the corresponding entries of $\mathbf{V}$; $Y_{n,k}$ is the (n,k)-th entry of the bus admittance matrix $\mathbf{Y} \in \mathbb{C}^{N_{bus}\times N_{bus}}$; $S_k \in \mathbb{C}$ is the complex apparent power at bus k; superscript star $\star$ represents the conjugate operator.

Separating the real and imaginary parts of Equation (2) gives the two equations about a PQ bus

$$\begin{aligned} P_k &= V_{d,k} \sum_{n=1}^{N_{bus}} \left(G_{n,k} V_{d,n} - B_{n,k} V_{q,n}\right) \\ &\quad + V_{q,k} \sum_{n=1}^{N_{bus}} \left(G_{n,k} V_{q,n} + B_{n,k} V_{d,n}\right) \qquad (3a) \\ Q_k &= V_{q,k} \sum_{n=1}^{N_{bus}} \left(G_{n,k} V_{d,n} - B_{n,k} V_{q,n}\right) \\ &\quad - V_{d,k} \sum_{n=1}^{N_{bus}} \left(G_{n,k} V_{q,n} + B_{n,k} V_{d,n}\right) \qquad (3b) \end{aligned}$$

where $P_k \le 0$ and $Q_k \le 0$[5] are the fixed active and reactive power loads at bus k; $G_{n,k}$ and $B_{n,k}$ are the (n,k)-th entries of the bus conductance matrix $\mathbf{G}$ and the bus susceptance matrix $\mathbf{B}$[6]; $V_{d,k}$, $V_{d,n}$, $V_{q,k}$ and $V_{q,n}$ are the corresponding entries of $\mathbf{V}_d$ and $\mathbf{V}_q$, which are unknown variables that should be determined.

For the PV bus we have

$$\begin{aligned} P_k &= V_{d,k} \sum_{n=1}^{N_{bus}} \left(G_{n,k} V_{d,n} - B_{n,k} V_{q,n}\right) \\ &\quad + V_{q,k} \sum_{n=1}^{N_{bus}} \left(G_{n,k} V_{q,n} + B_{n,k} V_{d,n}\right) \qquad (4a) \\ V_{m,k}^2 &= V_{d,k}^2 + V_{q,k}^2 \qquad (4b) \end{aligned}$$

where P_k is a fixed active power injection at bus k which is usually positive but can be negative; $V_{m,k}$ is the fixed voltage magnitude at bus k.

For the slack bus with an angle reference we have

$$\begin{aligned} V_{m,s}^2 &= V_{d,s}^2 + V_{q,s}^2 \qquad (5a) \\ 0 &= V_{q,s} \qquad (5b) \end{aligned}$$

where subscript s is the slack bus number; $V_{m,s}$ is the slack bus voltage magnitude.

One can further substitute (5b) in (5a), (4) and (3) to eliminate $V_{q,s}$. Finally, (3), (4), and (5) together are the power flow equations we will investigate in this paper. Note that they are in quadratic form, thus can be written succinctly as

$$PF(\mathbf{U}) := \{f_i(\mathbf{U}) = \mathbf{U}^T \mathbf{M}_i \mathbf{U} - r_i,\ i = 1, \cdots, 2N_{bus}\} \tag{6}$$

where $\mathbf{U} := [\mathbf{V}_d^T \ \mathbf{V}_q^T]^T$ is the unknown variable vector; $\mathbf{M}_i \in \mathbb{SR}^{2N_{bus}\times 2N_{bus}}$ is a symmetric constant matrix for the quadratic part; $r_i \in \mathbb{R}$ is the constant scalar part.

B. EQUIVALENT CURVE DESIGN OF ELLIPTICAL FORMULATION OF POWER FLOW EQUATIONS

We start our discussion with a given invertible linear map $\mathscr{E} \in \mathbb{R}^{2N_{bus}\times 2N_{bus}}$ that sends Equation (6) to a set of high dimensional ellipses $EF(\mathbf{U})$. The construction of $\mathscr{E}$ can be found in [20], [21]. Consider

$$\mathscr{E} : PF(\mathbf{U}) \to EF(\mathbf{U})$$

with

$$EF(\mathbf{U}) := \{g_i(\mathbf{U}) = \mathbf{U}^T \mathbf{H}_i \mathbf{U} - \gamma_i,\ i = 1, \cdots, 2N_{bus}\}$$

where $\mathbf{H}_i \in \mathbb{SR}^{2N_{bus}\times 2N_{bus}}$ and $\mathbf{H}_i \succ 0$; $\gamma_i > 0$.

Let $\mathscr{Z}(h; x)$ be the operator that takes the projection of $\{(x,y)|h(x,y) = 0\}$ onto x; define

$$\begin{aligned} EF_{l-}(\mathbf{U}) &:= EF(\mathbf{U}) - \{g_l(\mathbf{U})\} \\ EF_{l,\alpha}(\mathbf{U},\alpha) &:= EF_{l-}(\mathbf{U}) \cup \{g_l(\mathbf{U}) - \alpha,\ \alpha \in \mathbb{R}\}. \end{aligned}$$

Since $EF(\mathbf{U})$ defines a determined algebraic system, its algebraic set is generically 0-dimensional in $\mathbb{R}^{2N_{bus}}$. By removing one equation from $EF(\mathbf{U})$, $EF_{l-}(\mathbf{U})$ acquires one degree of freedom and defines a 1-dimensional algebraic set in $\mathbb{R}^{2N_{bus}}$. On the other hand, adding one extra degree of freedom to $EF(\mathbf{U})$ makes the algebraic set of $EF_{l,\alpha}(\mathbf{U},\alpha)$ 1-dimensional in $\mathbb{R}^{2N_{bus}+1}$. The following Lemma 1 shows an equivalence between these two 1-dimensional algebraic sets.

Lemma 1:

$$\mathscr{Z}(EF_{l-}; \mathbf{U}) = \mathscr{Z}(EF_{l,\alpha}; \mathbf{U})$$

The proof is trivial and omitted here. Next, we state the equivalent curve design of elliptical formulation in Theorem 1.

Theorem 1:

$$\mathscr{Z}(EF_{l-}; \mathbf{U}) = \mathscr{Z}\left(\{PF(\mathbf{U}) - \alpha \mathscr{E}^{-1}\mathbf{e}_l\}; \mathbf{U}\right)$$

where $\mathbf{e}_l \in \mathbb{R}^{2N_{bus}}$ is a unit column vector with the j-th entry being 1.

Proof: By definition, $EF_{l,\alpha}(\mathbf{U},\alpha)$ can also be expressed as $\{EF(\mathbf{U}) - \alpha\mathbf{e}_l\}$. Then we have

$$\begin{aligned} \mathscr{E}^{-1}\left(EF(\mathbf{U}) - \alpha\mathbf{e}_l\right) &= \mathscr{E}^{-1}\left(EF(\mathbf{U})\right) - \alpha\mathscr{E}^{-1}\mathbf{e}_l \\ &= PF(\mathbf{U}) - \alpha\mathscr{E}^{-1}\mathbf{e}_l. \end{aligned}$$

Since $\mathscr{E}$ is an invertible linear map, it is a homeomorphism. Hence,

$$\mathscr{Z}(EF_{l,\alpha}; \mathbf{U}) = \mathscr{Z}\left(\{PF(\mathbf{U}) - \alpha\mathscr{E}^{-1}\mathbf{e}_l\}; \mathbf{U}\right).$$

[5]Usually a load absorbs reactive power, but it can possibly generate reactive power. In that case $Q_k \ge 0$.

[6]$\mathbf{Y} = \mathbf{G} + j\mathbf{B}$

Finally, by Lemma 1 we conclude that

$$\mathscr{Z}(EF_{l-};\mathbf{U}) = \mathscr{Z}\big(\{PF(\mathbf{U}) - \alpha\mathscr{E}^{-1}\mathbf{e}_l\};\mathbf{U}\big).$$

□

III. HOLOMORPHIC EMBEDDING TECHNIQUE

Theorem 1 states that the 1-dimensional curves derived from the elliptical formulation EF_{l-} can be acquired alternatively from a particular parameterized power flow problem $PF(\mathbf{U}) - \alpha\mathscr{E}^{-1}\mathbf{e}_l$. In Section II, this α is restricted to a real-valued scalar to support one extra degree of freedom. If we allow α to be a complex number, the parameterized curve resides in the complex plane and becomes a 2-dimensional surface in the real space. If this complex-value parameterized curve happens to be governed by holomorphic functions, it is called the holomorphic embedding. The advantage of being holomorphic is that the global information of the embedded curve is determined and singularities on the curve can be predicted by analytic continuation techniques.

A. HOLOMORPHIC EMBEDDING OF POWER FLOW EQUATIONS

1) PQ BUS EMBEDDING

We start with the basic complex power balance equation for PQ bus in Equation (2). Note that $S_k = P_k + jQ_k$ we define

$$P_k(\alpha) := (1 + K_{p,k}\alpha)P_{k,0} \tag{8a}$$
$$Q_k(\alpha) := (1 + K_{q,k}\alpha)Q_{k,0} \tag{8b}$$

where $\alpha \in \mathbb{C}$; $K_{p,k}$ and $K_{q,k}$ are obtained from $\mathscr{E}^{-1}\mathbf{e}_l$ for some l; $P_{k,0}$ and $Q_{k,0}$ are the fixed starting active and reactive power which admit a known solution.

If we define a new variable $W_k := V_k^{-1}$ for $V_k \neq 0$, and restrict parameterized $W_k(\alpha)$ to be reflective such that $W_k(\alpha) = W_k(\alpha^\star)$, then Equation (2) can be written as

$$\sum_{n=1}^{N_{bus}} Y_{n,k}V_n(\alpha) = \Big((1 + K_{p,k}\alpha)P_{k,0} - j(1 + K_{q,k}\alpha)Q_{k,0}\Big)W_k^\star(\alpha^\star) \tag{9a}$$
$$V_k(\alpha)W_k(\alpha) = 1 \tag{9b}$$

Note that on the right hand side of (9a) we use $W_k^\star(\alpha^\star)$ instead of $W_k^\star(\alpha)$ since they are equal by the reflective property.[7]

Since $V_k(\alpha)$ and $W_k(\alpha)$ are holomorphic [38], we can use power series to represent them. Then, (9) can be re-written as

$$\sum_{n=1}^{N_{bus}}\Big(Y_{n,k}\sum_{i=0}^{\infty}v_{n,i}\alpha^i\Big) = \Big((1 + K_{p,k}\alpha)P_{k,0} - j(1 + K_{q,k}\alpha)Q_{k,0}\Big)\sum_{i=0}^{\infty}w_{n,i}^\star\alpha^i \tag{10a}$$

[7] A more detailed discussion on the reflective requirement can be found in [38].

$$\sum_{i=0}^{\infty}v_{n,i}\alpha^i\sum_{i=0}^{\infty}w_{n,i}\alpha^i = 1 \tag{10b}$$

where $v_{n,i}$ and $w_{n,i}$ are the power series coefficients.

Matching up coefficients for every monomial of α in (10a) and (10b) we can solve $(v_{k,1}, v_{k,2}, \cdots)$ and $(w_{k,1}, w_{k,2}, \cdots)$ recursively as long as $v_{k,0}$ and $w_{k,0}$ are provided.

2) PV BUS EMBEDDING

Next, we consider the holomorphic embedding for PV bus equations. To retain holomorphicity, we need to bring back the reactive power balance equation (3b) to (4) and consider reactive power input as a new variable. Again, by defining $W_k := V_k^{-1}$ for $V_k \neq 0$ and restricting parameterized $W_k(\alpha)$ to be reflective we have the holomorphic embedded equations

$$\sum_{n=1}^{N_{bus}} Y_{n,k}V_n(\alpha) = \Big((1+K_{p,k}\alpha)P_{k,0} - jQ_k(\alpha)\Big)W_k^\star(\alpha^\star) \tag{11a}$$
$$V_k(\alpha)V_k^\star(\alpha^\star) = V_{k,m}^2 + K_{v,k}\alpha \tag{11b}$$
$$V_k(\alpha)W_k(\alpha) = 1 \tag{11c}$$

where $V_{k,m} \in \mathbb{R}$ is the fixed voltage magnitude at bus k; $K_{v,k}$ is obtained from the corresponding entry of $\mathscr{E}^{-1}\mathbf{e}_l$.

By the holomorphic structure, we represent parameterized unknowns $V_n(\alpha)$, $W_k(\alpha)$, and $Q_k(\alpha)$ through their power series. Then, (11) are re-written as

$$\sum_{n=1}^{N_{bus}}\Big(Y_{n,k}\sum_{i=0}^{\infty}v_{n,i}\alpha^i\Big) = \Big((1 + K_{p,k}\alpha)P_{k,0} - j\sum_{i=0}^{\infty}q_{k,i}\alpha^i\Big)\sum_{i=0}^{\infty}w_{n,i}^\star\alpha^i \tag{12a}$$
$$\sum_{i=0}^{\infty}v_{n,i}\alpha^i\sum_{i=0}^{\infty}v_{n,i}^\star\alpha^i = V_{k,m}^2 + K_{v,k}\alpha \tag{12b}$$
$$\sum_{i=0}^{\infty}v_{n,i}\alpha^i\sum_{i=0}^{\infty}w_{n,i}\alpha^i = 1 \tag{12c}$$

where $q_{k,i}$'s are the power series coefficients of $Q_k(\alpha)$.

Matching up coefficients for every monomial of α in (12a), (12b) and (12c) we can solve u_i, w_i, and q_i as well.

3) SLACK BUS EMBEDDING

Consider the slack bus voltage magnitude equation (5a). Its holomorphic embedded equation is

$$V_s(\alpha)V_s^\star(\alpha^\star) = V_{s,m}^2 + K_s\alpha \tag{13}$$

where $V_{s,m}$ is the slack bus voltage magnitude, K_s is the corresponding entry from $\mathscr{E}^{-1}\mathbf{e}_l$.

Substituting the power series of $V_s(\alpha)$ into Equation (13) and matching up each monomial of α we have

$$v_{s,i} = -\Big(\sum_{n=1}^{i-1}v_{s,n}v_{s,i-n}\Big)/(2v_{s,0}) \text{ for } i \geq 2 \tag{14a}$$
$$v_{s,1} = K_s/(2v_{s,0}) \tag{14b}$$

Combining the corresponding equations from the PQ bus, PV bus and slack bus equations we finally solve the power series coefficients for each degree-i. In practice, every degree requires solving a real-valued linear system (sparse) with its size $(4N_{bus} + N_{gen} - 3) \times (4N_{bus} + N_{gen} - 3)$ where N_{gen} is the number of PV nodes. As i goes to infinity, the power series converges to the actual curve in the convergence range. To compromise accuracy and speed, we usually stop at a given maximum degree i_{max}.[8]

B. PADÉ APPROXIMATION

The above subsection shows that each node voltage (as well as reactive power at PV bus) can be embedded as a holomorphic function, and demonstrates a recursive way to obtain the coefficients. In practice the holomorphic function can only be evaluated by a finite sequence of power series. Thus, the accuracy of the sequence deteriorates when approaching the singularities of the holomorphic function. To achieve a better convergence performance and to predict the location of singular point, we further compute the Padé approximation. It approximates the holomorphic function by a rational function in which the numerator and denominator are polynomials. According to [39], [40], the Padé approximation has the maximum convergent domain if the degrees of its numerator and denominator have the minimum difference. It provides a criterion for determining the best degree(s) that should be chosen.

Consider an embedded voltage variable $v_k(\alpha)$ for some k. Suppose its first N coefficients are known.

$$v_k(\alpha) = \sum_{n=0}^{\infty} v_{k,n}\alpha^n \approx \sum_{n=0}^{N} v_{k,n}\alpha^n \tag{15}$$

Let its Padé approximation be

$$\sum_{n=0}^{N} v_{k,n}\alpha^n = \sum_{n=0}^{N_n} u_{k,n}\alpha^n \Big/ \sum_{n=0}^{N_d} l_{k,n}\alpha^n \tag{16}$$

where we specify $N_n + N_d = N$, $N_n \geq N_d$, and $N_n - N_d \leq 1$.

To reach a unique coefficient set, let $l_{k,0} = 1$. Matching up the coefficients for each monomial, we can solve $u_{k,n}$'s and $l_{k,n}$'s in a $(N+1) \times (N+1)$ complex-valued sparse linear system. If we compute the power series to the maximum degree i_{max}, the system size in the real space is $2(i_{max}+1) \times 2(i_{max}+1)$.

Once the Padé approximation has been calculated, we can move along the parameterized curve by evaluating Padé approximated values until a power mismatch threshold[9] has been reached. We can also compute the real-valued zeros to the denominator function of Padé. These zeros reveal the locations of singularities on the parameterized curve, which can further assist us designing appropriate arc length for passing through these singular points by the traditional predictor-corrector algorithm. Next section will discuss these designs in detail.

[8] [25] claims that degree i will deplete double precision digits after 60. How to choose an appropriate i_{max} is beyond the scope of this paper. We choose $i_{max} = 15$ in our numerical experiments by empirical experience considering speed and accuracy.

[9] In our numerical experiments, this threshold is set at 10^{-3} p.u.

Algorithm 1 Outer Loop for Locating Power Flow Solutions

```
Solving for a power flow solution x_1.
Generating elliptical mapping 𝒪 by algorithms in [20], [21].
S ← x_1                                  ▷ Initialize solution set
N_solu ← |S|                             ▷ Initialize number of solutions
k ← 0                                    ▷ Initialize counting number
while k ≠ N_solu do
    k ← k + 1                            ▷ Update counting number
    x_0 ← x_k                            ▷ Update starting solution
    for l = 1, 2, ··· , N_eqn do
        Compute 𝒪^{-1} e_l               ▷ Equivalent curve design
        Algorithm 2                      ▷ HEBC Algorithm
        Return S_new                     ▷ Return newly found solutions
        if S_new is not in S then
            S ← S ∪ S_new                ▷ Update the solution set
            N_solu ← |S|                 ▷ Update the number of solutions
        end if
    end for
end while
```

IV. HOLOMORPHIC EMBEDDING BASED CONTINUATION METHOD

The proposed HEBC method can be divided into an outer loop part and an inner loop part. The outer loop focuses on new solution updates and sequential curve designs; while the inner loop primarily follows the curve fed by the outer loop and returns the solution set found on that curve.

A. OUTER LOOP FOR SOLUTION SEARCH

To make this article self-sustained, we briefly explain the search strategies in the outer loop and summarize it in Algorithm 1. Interested readers can refer to [20].

We start Algorithm 1 with a known solution x_1 which can be solved by Newton's method or other techniques.[10] After several initialization steps, designing the curve $\{PF - \alpha\mathscr{O}^{-1}\mathbf{e}_l\}$ which is equivalent to $\{EF_{l-}\}$ for l. Following the curve from $l = 1$ to the last one by Algorithm 2 (which will be discussed shortly below) and collect new solutions. When finished tracing curves, assigning the starting point x_0 to a newly found solution, say, x_2, and repeating the procedure. The whole loop terminates upon every solution having been assigned to a starting point. Algorithm 1 presents a procedure to follow each curve sequentially. However, the curve designs at the same starting solution are independent with each other, suggesting a parallel computing framework to simultaneously trace these curves. The parallel computing is not performed

[10] This step relies on the past extensive research of solving a high voltage solution to the power flow problem. Many mature solvers are able to do this job for very large systems.

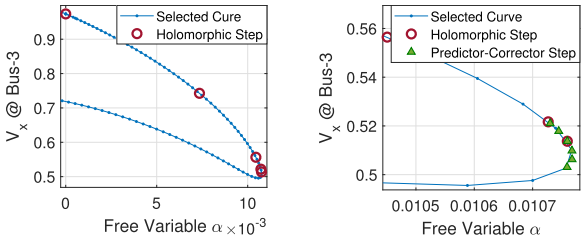

(a) Holomorphic Steps (b) Predictor-Corrector Steps

FIGURE 1. Holomorphic Steps and Preditor-Corrector Steps.

in this article, but can be done with ease and increase speed drastically.

B. INNER LOOP FOR CURVE TRACING

Instead of tracing a curve by the traditional predictor-corrector algorithm, we apply the holomorphic embedding technique to quickly pass through the regular curve segments. The predictor-corrector algorithm is only executed for traveling across singularities. It is switched back to the holomorphic embedding as soon as current steps leave a singular point.

Figure 1(a) shows four holomorphic steps on a selected curve from a 5-bus case [13]. They reach the singular point very quickly. On the other hand, the blue curve in Figure 1(a) was generated by the traditional predictor-corrector algorithm. It took dozens of steps to reach the same singularity.

1) CRITERION TO ENTER PREDICTOR-CORRECTOR ROUTINE

Two indicators are considered to trigger the switch of the algorithms in Algorithm 2. The first indicator appears when the corrector steps fail to make the holomorphic prediction converge within a certain number of iterations. Another indicator comes when $|\alpha_{k_h+1} - \alpha_{k_h}|$ is smaller than a threshold value $d\alpha_{h,min}$. Both suggest that current holomorphic step is close to singular (or at least badly scaled with respect to α).

2) USING A WARM STARTER TO ACCELERATE PREDICTOR-CORRECTOR STEPS

One can initiate the predictor-corrector routine from a minimum step size, and increase it gradually. We refer it to a *cold starter*. To avoid slow "warming up" steps, a warm starter is proposed and implemented. It relies on an estimated distance d_{hp} from the singular point to the last holomorphic point. We specifically choose the initial step interval S_{pc} to be $1/5$ of the estimated distance d_{hp} and to be no greater than 0.45 of the last holomorphic step size. Then, using S_{pc} to compute two backward steps to initiate a quadratic predictor. For example, the first two green triangles on the upper curve segment in Figure 1(b) are the backward points evaluated by Padé approximation at the step length S_{pc}. It makes the predictor-corrector routine quickly pass through the singular point as shown by the rest green triangles.

3) CRITERION TO EXIT PREDICTOR-CORRECTOR ROUTINE

When travelling across a singular point, the direction of curve changes. Numerically, there exists a particular step m_c such that $(\alpha_{m_c} - \alpha_{m_c-1})(\alpha_{m_c+1} - \alpha_{m_c}) < 0$. After this moment, we continue the predictor-corrector routine for a while until the curve's slope value returns from infinity back

Algorithm 2 Holomorphihc Embedding Based Continuation

Input selected curve $\mathscr{E}^{-1}\mathbf{e}_l$.
Initialize the $1st$ step.
for $k = 1 : M$ **do**
  for $k_h = 1 : N_h$ **do**
    Initialize the $1st$ holomorphic step size δ_h.
    Prepare parameters for holomorphic embedding.
    Compute power series of holomorphic embedding.
    Compute Padé approximation.
    Evaluate voltage values from Padé and update α_{k_h+1}.
    Evaluate power mismatch dP_{mis} from computed voltages.
    while minimum pole p_{min} is not determined **do**
      Compute roots $\{\zeta_i\}$ from Padé denominator.
      $p_{min} \leftarrow \zeta_{min}$ if the minimum real root ζ_{min} has correct sign.
    end while
    Increase δ_h while $dP_{mis} < dP_{max}$ and |current point| $< |p_{min}|$.
    Decrease δ_h while $dP_{mis} \geq dP_{max}$ or |current point| $\geq |p_{min}|$.
    Correct current holomorphic predicted point by Newton's method.
    if Correction succeeds **then**
      Record current point.
    else
      Delete current point and compute a starter for switching algorithm.
      Break.
    end if
    if $\alpha_{k_h+1}\alpha_{k_h} < 0$ **then**
      Find a solution nearby.
      if Fail to locate the solution **then**
        Delete current point and compute a cold starter for switching algorithm.
        Break.
      else
        Record solution to solution set S_{new}.
        Check completeness of the curve; jump out Algorithm 2 if completed.
      end if
    end if
    if $|\alpha_{k_h+1} - \alpha_{k_h}| < d\alpha_{h,min}$ **then**
      Compute a starter for switching algorithm.
      Break.
    end if
  end for
  Execute predictor-corrector routine.
end for
Return solution set S_{new}

to a tractable value. Instead of evaluating the actual slope of the curve, we monitor the maximum variable secant slope R_m.

$$R_m := max\{|(V_{k,m} - V_{k,m-1})/(\alpha_m - \alpha_{m-1})|,\ \forall k\} \quad (17)$$

As long as R_m drops to a threshold R_{max}, say, 2×10^4, we jump out of the predictor-corrector routine and start a new sequence of holomorphic steps.

C. COMPUTATIONAL COMPLEXITY COMPARISON

The holomorphic prediction consists of two sub-routines: 1) construct the power series; 2) compute Padé approximation based on the power series. Both sub-routines require solving sparse linear systems. The sparsity reduces computational efforts in practice but makes analysis hard. To get a rough idea of the complexity, we simply assume the matrices are dense in the analysis, but solve them in sparse form practically.

In Section III computing the power series coefficients requires solving a sequence of linear systems up to the highest degree i_{max}. A favorable observation is that all these linear systems share the same constant matrix. Thus, the LU factorization only needs to be performed once, while forward and backward substitutions need to be performed i_{max} times to generate coefficients for all degrees. Therefore, the computational complexity for the power series is

$$C_{TI} = \frac{2}{3}\left(4N_{bus}+N_{gen}-3\right)^3+2\left(4N_{bus}+N_{gen}-3\right)^2 i_{max} \quad (18)$$

In Padé approximation, the complexity is

$$C_{Pd} = \left(\frac{2}{3}\left(2i_{max}+2\right)^3+2\left(2i_{max}+2\right)^2\right)\left(2N_{bus}-1\right) \quad (19)$$

The total complexity of a holomorphic prediction is $C_{Holo} = C_{TI} + C_{Pd}$.

On the other hand, in the traditional predictor-corrector algorithm the Newton's iterations in correctors are the most computational complex part. Again, suppose a dense Jacobian matrix (sparse in practice) the complexity of solving one Newton's iteration is

$$C_{Newton} = \frac{2}{3}\left(2N_{bus} - 1\right)^3 + 2\left(2N_{bus} - 1\right)^2 \quad (20)$$

Suppose i_{max} is fixed, $N_{gen} = 0.2N_{bus}$,[11] and each corrector takes 3 Newton's iterations to converge for both the holomorphic step and the traditional predictor-corrector step, we have

$$R = \lim_{N_{bus}\to\infty} \frac{C_{Holo} + 3C_{Newton}}{3C_{Newton}} = 4.087 \quad (21)$$

It suggests that one holomorphic step takes about four predictor-corrector steps computations asymptotically with the dense matrix LU factorization. So an average holomorphic step size which is greater than 4 times the average step size of the predictor-corrector algorithm can potentially reduce the computational time under the same assumptions.

[11]The number of PV buses usually occupies a small fraction of the total number of buses.

D. REMARK ON DISTRIBUTION SYSTEM POWER FLOW

Power flow convergence is one of the major challenges in modern distribution system analysis. As a non-iterative power flow method free of divergence issue in theory, HELM was initially proposed for three-phase balanced conditions, usually representing a transmission system. The development of HELM to three-phase unbalanced conditions can extend such a benefit to distribution systems [41], [42]. In addition, besides constant power load model, HELM can also be extended to consider ZIP load [43] and induction motor load [33]. These extensions can be directly integrated with the proposed HEBC without any theoretical difficulty.

In future distribution grids, reversal power flow would be a common phenomenon introduced by massive integration of distributed wind and solar PV generations. It should be noted that the reversal power flow can be fully represented by traditional power balance equations with power injections at load buses changed to small or even negative values. Such a change may affect the number and distribution of the power flow solutions as well as the run-time, while having no impact on the convergence of the proposed HEBC at all, see our recent work [44].

V. NUMERICAL EXPERIMENTS

This section presents a comprehensive numerical evaluation of the proposed HEBC method on several standard power system test cases including "case3TS", "case3", "case4gs","case4BBc", "case4BB0", "case5Salam", "case6ww", "case7Salam", "case9", "case14", "case30", "case33bw", "case39", "case57",[12] which can be found in the Matpower libary [45], and "case5loop" [19]. To avoid numerical instability and structurally unstable solutions, small resistance at 10^{-4} p.u. is added to lossless lines. The HEBC method and the full predictor-corrector method are coded in Matlab R2017b and executed on a PC with 2.8GHz Intel i7-7700HQ CPU and 16GB RAM.

A. COMPARISON TO HOMOTOPY CONTINUATION METHOD

To demonstrate the superiority of computational efficiency in finding multiple power flow solutions, we begin with a comparison of the proposed HEBC method to the homotopy continuation method. The homotopy continuation is performed by the PHCpack [46].

The HEBC method finds all the actual power flow solutions in this comparison as well as case14.[13] Figure 2 shows execution time (in logarithmic scale) comparison between two methods. For test cases smaller than 5 buses, the PHCpack runs faster than the proposed HEBC method. However, for cases more than 5 buses, the HEBC outperforms the homotopy continuation method substantially. Considering the HEBC method is coded in Matlab and is not optimized

[12]Tap ratios are removed in this case to reduce the number of solutions.

[13]No existing literature claims complete solution sets for larger IEEE test cases.

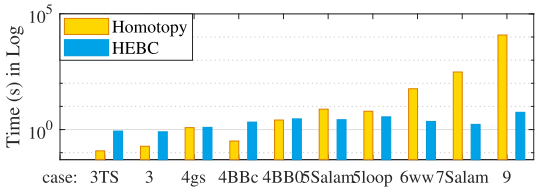

FIGURE 2. Comparison Between Homotopy Continuation and HEBC.

TABLE 1. Numerical results by predictor-corrector method.

Method	Predictor-Corrector		
Case	overall steps	overall time (s)	# Solutions
3TS	2962	1.257	6
3	3349	1.143	6
4gs	4281	1.405	6
4BBc	8838	2.660	12
4BB0	13791	3.719	14
5Salam	11465	3.626	10
5loop	17049	4.568	10
6ww	9421	3.209	6
7Salam	5195	1.978	4
9	22264	10.945	8
14	151423	102.401	30
30	5358518	6054.987	472
33bw	311957	249.736	16
39	3009935	3758.195	176
57	14647351	23864.005	606

TABLE 2. Numerical results by HEBC method.

Method	HEBC				
Routine	Holomorphic		Predictor-Corrector		overall
Case	# steps	time (s)	# step	time (s)	time (s)
3TS	253	0.373	228	0.133	0.859
3	290	0.345	387	0.155	0.798
4gs	481	0.625	766	0.197	1.248
4BBc	850	1.174	1358	0.362	2.102
4BB0	1212	1.489	2805	0.773	2.890
5Salam	1128	1.754	1224	0.290	2.661
5loop	1695	2.448	1627	0.358	3.537
6ww	995	1.402	1143	0.288	2.249
7Salam	564	1.068	362	0.132	1.676
9	1668	3.158	4026	1.668	5.572
14	13350	34.443	27238	12.784	50.013
30	403181	2077.966	910664	674.828	2813.249
33bw	15904	81.896	65351	43.519	129.323
39	184458	1247.794	1044166	930.796	2204.543
57	835550	10565.59	3078609	3598.361	14304.691

HEBC provides the same solution sets for all the cases as in Table I.

to reach the most computational performance, the time reductions from HEBC are impressive. Test cases larger than 9 buses cannot be solved by PHCpack within 24 hours, thus are not considered in this comparison.[14]

B. COMPARISON TO FULL PREDICTOR-CORRECTOR ALGORITHM

In this part, we testify the traditional full predictor-corrector method from [20] and the proposed HEBC method on the same set of test cases, and compare their numerical performances. Both methods provide the same solution sets for

[14] A more recent progress in [16] successfully reduced the computational time of case14 to 5 minutes, however, the proposed HEBC is still much faster.

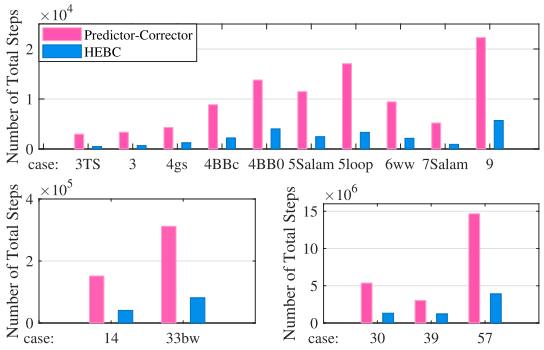

FIGURE 3. Steps needed for different cases with full predictor-corrector and HEBC.

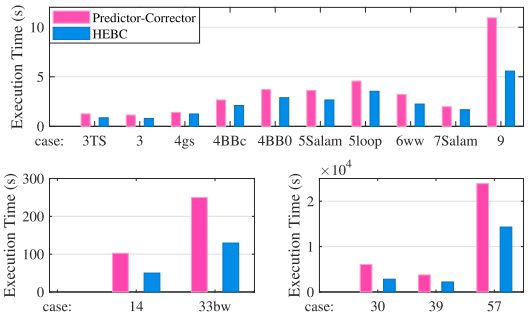

FIGURE 4. Execution times with full predictor-corrector and HEBC.

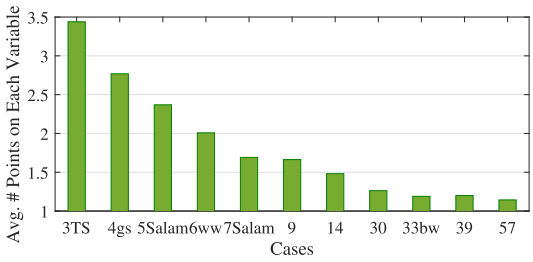

FIGURE 5. Equivalent no. random seeds for each variable.

all cases, but the HEBC method is more efficient than the traditional predictor-corrector method. Some hard[15] sample curves are presented in Appendix. One can see from the left plots of Figure 6 that the traditional full predictor-corrector method, though with quadratic predictor and automatic step length adaption, takes very dense points to trace curves. On the other hand, the right plots of Figure 6 are primarily sparse. Small dense point periods only occur around singularities when HEBC switches to the predictor-corrector routine for passing through those singularities. Summaries of the numerical results are collected in Table 1 and 2. Sample curves from simulations are provided in Figure 6.

Comparing the results in Figure 3, the total number of steps for HEBC is about 1/6 to 1/3 of the total number of steps for the full predictor-corrector method. This ratio, not surprisingly, should depend on the problem structure.

[15] A curve is hard to follow in the sense that it contains too many singularities or some singular points are very sharp when turning directions.

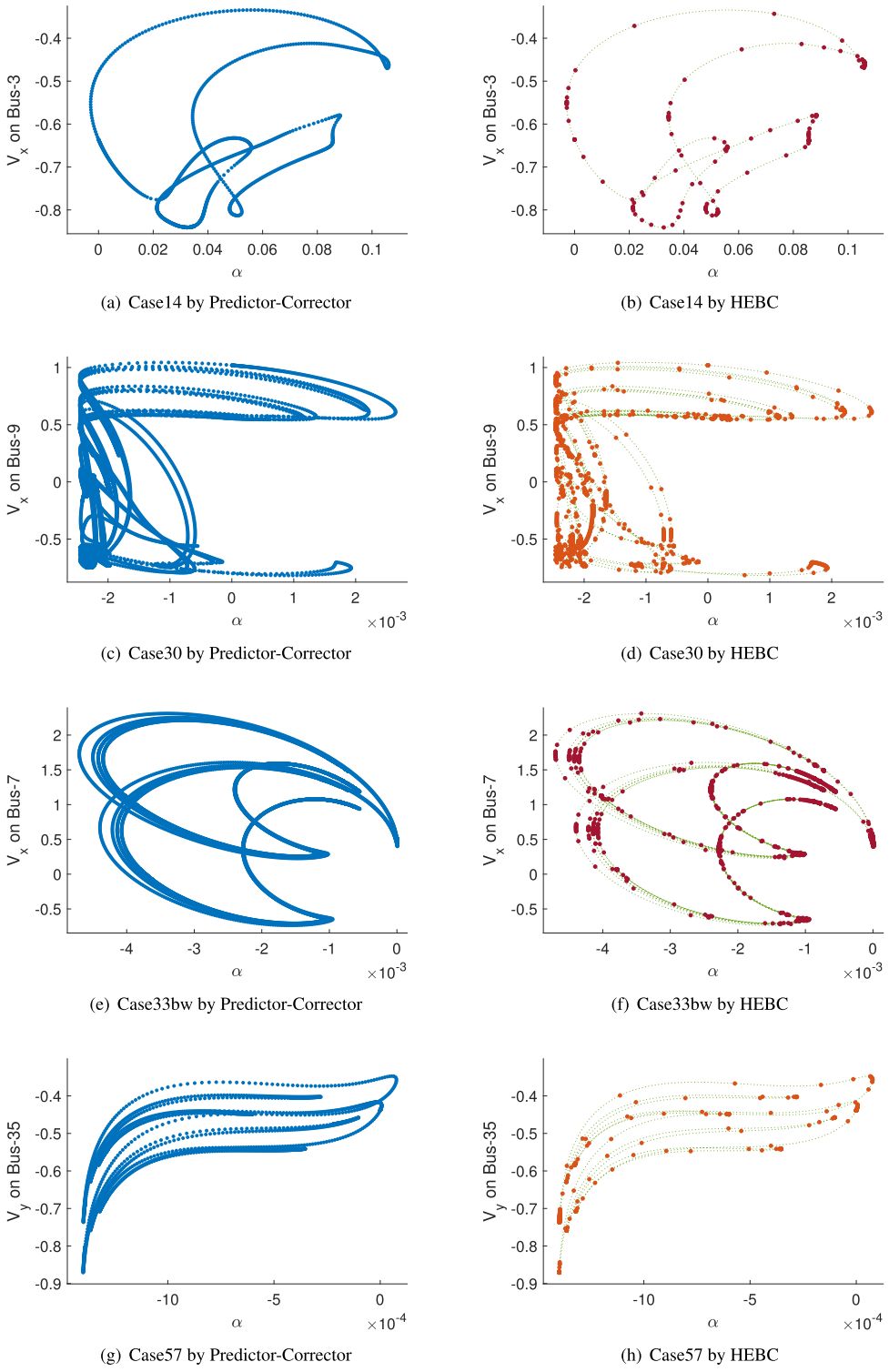

(a) Case14 by Predictor-Corrector (b) Case14 by HEBC

(c) Case30 by Predictor-Corrector (d) Case30 by HEBC

(e) Case33bw by Predictor-Corrector (f) Case33bw by HEBC

(g) Case57 by Predictor-Corrector (h) Case57 by HEBC

FIGURE 6. Sample curves followed by predictor-corrector (Left) and HEBC (Right).

In general, fewer singularities and longer horizontal curve segments favor the HEBC more.

To reveal the efficiency of HEBC, we compute the equivalent number of predictor-corrector steps N_{eqv}

$$N_{eqv} := (N_{pc} - N_{he,pc})/N_{he,holo} \tag{22}$$

where N_{pc} is the number of full predictor-corrector steps; $N_{he,pc}$ is the number of predictor-corrector routine steps in HEBC; and $N_{he,holo}$ is the number of holomorphic routine steps in HEBC. From Table 1 and 2 we calculate that one holomorphic step on average can represent 8.5 predictor-corrector steps, with the worst case of 7 steps and

the best case of 15 steps. In Figure 4 the first 9 small cases up to case7Salam show a limited time saving by HEBC. However, starting at case9 the HEBC method outperforms the full predictor-corrector method by up to 50% of the execution time. Larger cases also exhibit at least 30% time saving in the lower plots of Figure 4.

C. AVERAGE NUMBER OF STEPS ON EACH DIMENSION

Recall that the HEBC method calls the Newton's method at each step to correct the predicted point. These predicted points are sequentially determined over the curve tracing process. Thus, the HEBC method can be regarded as a systematic way to choose initial points for solving the power flow equations, where the number of initial points equals the number of steps in Table 2, i.e. the sum of entries in the second and forth columns for each case. From this point of view, one can assess the efficiency of HEBC by computing the average number of initial points (or steps) allocated in each dimension

$$R_{eq} := N^{1/d} \tag{23}$$

where N is the total number of initial points, d is the dimensionality of the problem. R_{eq} represents the number of points required in each single dimension such that the total number of initial points composed by their direct combinations achieves the same amount of initial points N for the whole d-dimensional problem. Specifically for our problem, R_{eq} is computed as

$$R_{eq} = (N_{he,pc} + N_{he,holo})^{1/(2N_{bus}-1)} \tag{24}$$

Figure 5 depicts the trend of R_{eq} as system size increases. One can clearly see that the average number of steps distributed on each dimension decreases to nearly 1. Hence, despite the increase of total number of steps, the average number of steps on each dimension seems to decrease in an asymptotic sense.

VI. CONCLUSIONS

In this paper, we proposed an efficient hybrid method to solve multiple power flow solutions. We derived an equivalent curve design to the elliptical formulation of the power flow equations. Based on this design, a holomorphic embedding continuation method was introduced to replace the traditional predictor-corrector algorithm for regular curve tracing. Singular points were passed by the predictor-corrector routine. The complexity of one holomorphic step is around four times the complexity of a predictor-corrector step under certain assumptions. Numerical simulations showed that one holomorphic step size is equivalent to over eight predictor-corrector step size on average, and saved up to half of the computational time for some large test cases.

Investigation on the distribution of multiple power flow solutions and how they change over discrete events are our ongoing research [44]. A possible future direction of research can use the proposed method to find multiple power flow solutions for dynamic stability analysis, especially in characterizing the stability boundary of a stable equilibrium point. Another interesting topic would be using this method for solving optimal power flow problems.

ACKNOWLEDGMENT

The authors would like to acknowledge the helpful discussions with Dr. Wenqiang Feng from DST Systems, Dr. Honghao Zheng from Siemens, Prof. Konstantin Turitsyn at MIT and Prof. Bernard Lesieutre at UW-Madison.

REFERENCES

[1] M. Pai, *Energy Function Analysis for Power System Stability*. New York, NY, USA: Springer, 2012.
[2] H.-D. Chiang, *Direct Methods for Stability Analysis of Electric Power Systems: Theoretical Foundation, BCU Methodologies, and Applications*. Hoboken, NJ, USA: Wiley, 2011.
[3] P. W. Sauer and M. A. Pai, *Power System Dynamics and Stability*, vol. 101. Upper Saddle River, NJ, USA: Prentice-Hall, 1998.
[4] A. Klos and J. Wojcicka, "Physical aspects of the nonuniqueness of load flow solutions," *Int. J. Elect. Power Energy Syst.*, vol. 13, no. 5, pp. 268–276, 1991.
[5] B. K. Johnson, "Extraneous and false load flow solutions," *IEEE Trans. Power App. Syst.*, vol. PAS-96, no. 2, pp. 524–534, Mar. 1977.
[6] Y. Tamura, Y. Nakanishi, and S. Iwamoto, "On the multiple solution structure, singular point and existence condition of the multiple load-flow solutions," *IEEE Trans. Power App. Syst.*, vol. 99, no. 4, p. 1322, Jan. 1980.
[7] H.-D. Chiang and M. E. Baran, "On the existence and uniqueness of load flow solution for radial distribution power networks," *IEEE Trans. Circuits Syst.*, vol. 37, no. 3, pp. 410–416, Mar. 1990.
[8] A. J. Korsak, "On the question of uniqueness of stable load-flow solutions," *IEEE Trans. Power App. Syst.*, vol. PAS-91, no. 3, pp. 1093–1100, May 1972.
[9] H. D. Nguyen and K. S. Turitsyn, "Appearance of multiple stable load flow solutions under power flow reversal conditions," in *Proc. IEEE PES General Meeting Conf. Expo.*, Jul. 2014, pp. 1–5.
[10] W. Feng, J. Wu, C. Yuan, G. Liu, R. Dai, Q. Shi, and F. Li, "A graph computation based sequential power flow calculation for large-scale ACDC systems," 2019, *arXiv:1902.10192*. [Online]. Available: https://arxiv.org/abs/1902.10192
[11] D. Mehta, H. D. Nguyen, and K. Turitsyn, "Numerical polynomial homotopy continuation method to locate all the power flow solutions," *IET Gener., Transmiss. Distrib.*, vol. 10, no. 12, pp. 2972–2980, 2016.
[12] C. J. Tavora and O. J. Smith, "Equilibrium analysis of power systems," *IEEE Trans. Power App. Syst.*, vol. PAS-91, no. 3, pp. 1131–1137, May 1972.
[13] F. Salam, L. Ni, S. Guo, and X. Sun, "Parallel processing for the load flow of power systems: The approach and applications," in *Proc. 28th IEEE Conf. Decis. Control*, Dec. 1989, pp. 2173–2178.
[14] F. Salam, L. Ni, X. Sun, and S. Guo, "Parallel processing for the steady state solutions of large-scale non-linear models of power systems," in *Proc. IEEE Int. Symp. Circuits Syst.*, May 1989, pp. 1851–1854.
[15] J. Baillieul and C. Byrnes, "Geometric critical point analysis of lossless power system models," *IEEE Trans. Circuits Syst.*, vol. CS-29, no. 11, pp. 724–737, Nov. 1982.
[16] T. Chen and D. Mehta, "On the network topology dependent solution count of the algebraic load flow equations," *IEEE Trans. Power Syst.*, vol. 33, no. 2, pp. 1451–1460, Mar. 2018.
[17] W. Ma and J. S. Thorp, "An efficient algorithm to locate all the load flow solutions," *IEEE Trans. Power Syst.*, vol. 8, no. 3, pp. 1077–1083, Aug. 1993.
[18] O. Coss, J. D. Hauenstein, H. Hong, and D. K. Molzahn, "Locating and counting equilibria of the Kuramoto model with rank-one coupling," *SIAM J. Appl. Algebra Geometry*, vol. 2, no. 1, pp. 45–71, 2018.
[19] D. K. Molzahn, B. C. Lesieutre, and H. Chen, "Counterexample to a continuation-based algorithm for finding all power flow solutions," *IEEE Trans. Power Syst.*, vol. 28, no. 1, pp. 564–565, Feb. 2013.
[20] B. Lesieutre and D. Wu, "An efficient method to locate all the load flow solutions-revisited," in *Proc. 53rd Annu. Allerton Conf. Commun., Control, Comput. (Allerton)*, 2015, pp. 381–388.
[21] D. Wu, *Algebraic Set Preserving Mappings for Electric Power Grid Models and its Applications*. Madison, WI, USA: The Univ. of Wisconsin-Madison, 2017.

[22] D. Wu, D. K. Molzahn, B. C. Lesieutre, and K. Dvijotham, "A deterministic method to identify multiple local extrema for the ac optimal power flow problem," *IEEE Trans. Power Syst.*, vol. 33, no. 1, pp. 654–668, Jan. 2018.
[23] H. Schwetlick and J. Cleve, "Higher order predictors and adaptive steplength control in path following algorithms," *SIAM J. Numer. Anal.*, vol. 24, no. 6, pp. 1382–1393, 1987.
[24] C. Den Heijer and W. Rheinboldt, "On steplength algorithms for a class of continuation methods," *SIAM J. Numer. Anal.*, vol. 18, no. 5, pp. 925–948, 1981.
[25] A. Trias, "The holomorphic embedding load flow method," in *Proc. IEEE PES General Meeting*, Jul. 2012, pp. 1–8.
[26] P. Sauer, "Explicit load flow series and functions," *IEEE Trans. Power App. Syst.*, vol. PAS-100, no. 8, pp. 3754–3763, Aug. 1981.
[27] W. Xu, Y. Liu, J. C. Salmon, T. Le, and G. W. K. Chang, "Series load flow: A novel noniterative load flow method," *IEE Proc. Gener., Transmiss. Distrib.*, vol. 145, no. 3, pp. 251–256, May 1998.
[28] A. C. Z. D. Souza, C. B. R. Junior, B. I. L. Lopes, R. C. Leme, and O. A. S. Carpinteiro, "Non-iterative load-flow method as a tool for voltage stability studies," *IET Gener., Transmiss. Distrib.*, vol. 1, no. 3, pp. 499–505, May 2007.
[29] A. Trias and J. L. Marín, "The holomorphic embedding loadflow method for dc power systems and nonlinear DC circuits," *IEEE Trans. Circuits Syst. I, Reg. Papers*, vol. 63, no. 2, pp. 322–333, Feb. 2016.
[30] C. Liu, B. Wang, F. Hu, K. Sun, and C. L. Bak, "Online voltage stability assessment for load areas based on the holomorphic embedding method," *IEEE Trans. Power Syst.*, vol. 33, no. 4, pp. 3720–3734, Jul. 2017.
[31] S. D. Rao, D. J. Tylavsky, and Y. Feng, "Estimating the saddle-node bifurcation point of static power systems using the holomorphic embedding method," *Int. J. Elect. Power Energy Syst.*, vol. 84, pp. 1–12, Jan. 2017.
[32] C. Liu, K. Sun, B. Wang, and W. Ju, "Probabilistic power flow analysis using multidimensional holomorphic embedding and generalized cumulants," *IEEE Trans. Power Syst.*, vol. 33, no. 6, pp. 7132–7142, Nov. 2018.
[33] R. Yao, K. Sun, D. Shi, and X. Zhang, "Voltage stability analysis of power systems with induction motors based on holomorphic embedding," *IEEE Trans. Power Syst.*, vol. 34, no. 2, pp. 1278–1288, Mar. 2019.
[34] C. Liu, B. Wang, X. Xu, K. Sun, D. Shi, and B. C. L. Bak, "A multi-dimensional holomorphic embedding method to solve ac power flows," *IEEE Access*, vol. 5, pp. 25270–25285, 2017.
[35] B. Wang, C. Liu, and K. Sun, "Multi-stage holomorphic embedding method for calculating the power-voltage curve," *IEEE Trans. Power Syst.*, vol. 33, no. 1, pp. 1127–1129, Jan. 2017.
[36] Y. Feng and D. Tylavsky, "A holomorphic embedding approach for finding the type-1 power-flow solutions," *Electr. Power Energy Syst.*, vol. 102, pp. 179–188, Nov. 2018.
[37] F. D. Freitas, A. C. Santos, Jr., and L. F. J. Fernandes, and Y. G. I. Acle, "Restarted holomorphic embedding load-flow model based on low-order Padé approximant and estimated bus power injection," *Elect. Power Energy Syst.*, vol. 112, pp. 326–338, Nov. 2019.
[38] A. Trias, "Fundamentals of the holomorphic embedding load-flow method," Sep. 2015, *arXiv:1509.02421*. [Online]. Available: https://arxiv.org/abs/1509.02421
[39] H. Stahl, "On the convergence of generalized Padé approximants," *Construct. Approximation*, vol. 5, no. 1, pp. 221–240, 1989.
[40] H. Stahl, "The convergence of Padé approximants to functions with branch points," *J. Approximation Theory*, vol. 91, no. 2, pp. 139–204, 1997.
[41] B. V. Rao, F. Kupzog, and M. Kozek, "Three-phase unbalanced optimal power flow using holomorphic embedding load flow method," *Sustainability*, vol. 11, no. 6, pp. 1–16, 2019.
[42] Y. Ju, "Holomorphic embedding load flow modeling of the three-phase active distribution network," *Preprints*, pp. 1–7, 2018.
[43] S. S. Baghsorkhi and S. P. Suetin, "Embedding ac power flow in the complex plane part I: Modelling and mathematical foundation," 2016, *arXiv:1604.03425*. [Online]. Available: https://arxiv.org/abs/1604.03425
[44] D. Wu and B. Wang, "On distribution patterns of power flow solutions," *IEEE PES Lett.*, to be published.
[45] R. D. Zimmerman and C. E. Murillo-Sánchez. PSERC Cornell. *Matpower*. Accessed: Jul. 8, 2019. [Online]. Available: https://matpower.org/
[46] J. Verschelde, "Algorithm 795: PHCpack: A general-purpose solver for polynomial systems by homotopy continuation," *ACM Trans. Math. Softw. (TOMS)*, vol. 25, no. 2, pp. 251–276, 1999.
[47] D. Wu and B. Wang, "Power flow solution sets of standard IEEE test systems," *IEEE Dataport*, 2019. Accessed: Jul. 8, 2019. [Online]. Available: http://dx.doi.org/10.21227/24bh-hj72

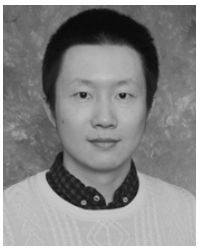

DAN WU (S'14–M'17) received the B.S. degree in electrical engineering and automation from the Huazhong University of Science and Technology, Wuhan, China, in 2012, and the M.S. and Ph.D. degrees from the University of Wisconsin-Madison, Madison, WI, USA, in 2014 and 2017, respectively. He is currently a Postdoctoral Associate with the Laboratory for Information and Decision Systems, Massachusetts Institute of Technology. His research includes nonlinear optimization, electric power system analysis, interdependent complex systems, algebraic and topological methods in engineering applications.

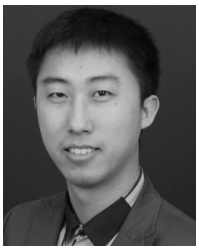

BIN WANG (S'14–M'18) received the B.S. and M.S. degrees from Xi'an Jiaotong University, in 2011 and 2013, respectively, and the Ph.D. degree from the University of Tennessee, Knoxville, TN, USA, in 2017, all in electrical engineering. He is currently a Postdoctoral Researcher with the Department of Electrical and Computer Engineering, Texas A&M University. His research interests include power system dynamics, stability, and control.